Sharp error estimates for a discretisation of the 1D convection/diffusion equation with Dirac initial data

Michael B. Giles
giles@comlab.ox.ac.uk

Oxford University Computing Laboratory, Oxford OX1 3QD

This paper derives sharp l_∞ and l_1 estimates of the error arising from an explicit approximation of the constant coefficient 1D convection/diffusion equation with Dirac initial data. The analysis embeds the discrete equations within a semi-discrete system of equations which can be solved by Fourier analysis. The error estimates are then obtained though asymptotic approximation of the integrals resulting from the inverse Fourier transform. This research is motivated by the desire to prove convergence of approximations to adjoint partial differential equations.

1 Introduction

This paper is concerned with a detailed error analysis of a particularly simple problem, a forward Euler central space discretisation of the one-dimensional constant coefficient convection/diffusion equation on an infinite domain with Dirac initial data. The analytic approach which is followed, embedding the discrete equations within a semi-discrete system of equations which can be analysed by Fourier transformation, is based on the approach used by Brenner, Thomée and Wahlbin [3]. However, their interest was in studying convergence for L_p initial data, as opposed to the Dirac initial data of interest in this paper.

The reason for the focus on Dirac initial data is concern with the convergence of adjoint discretisations. Adjoint methods are being used heavily for optimal design [8, 9], error analysis and correction for integral outputs [10, 6, 1], and optimal grid adaptation [2, 4]. In applications in which the original p.d.e. is nonlinear, the adjoint discretisation is usually obtained in one of two ways, either as a discretisation of the adjoint p.d.e. corresponding to the linearisation of the original p.d.e., or as the transposed equation corresponding to the linearised discretisation of the original p.d.e. In either case, if the original nonlinear solution is smooth, then the coefficients of the adjoint discretisation will be smooth, and it is possible to prove convergence in both steady and unsteady applications as the mesh spacing and timestep approach zero [11, 12]. However, when the underlying nonlinear solution is discontinuous, as in the case of shocks in compressible flow, then there is numerical evidence [5] showing that one must be careful in the treatment of the discontinuity to obtain convergence for the adjoint discretisation.

To understand the connection between Dirac initial data and adjoint equations, consider the following system of linear equations,

$$U^{n+1} = A^n U^n,$$

arising from the discretisation of an unsteady linear one-dimensional p.d.e. Here U^n represents the approximation to a scalar variable $u(x,t)$ on a one-dimensional grid with uniform spacing h at time $t^n = nk$. If one is interested in the value of an integral output

$$J = \int_{-\infty}^{\infty} g(x)\, u(x,T)\, \mathrm{d}x,$$

this may be approximated as

$$J_h = h \sum_j g(x_j)\, U_j^N,$$

where $T = Nk$. Alternatively, but equivalently, it can be evaluated as

$$J_h = h \sum_j V_j^0\, U_j^0,$$

where the adjoint solution V_j^n satisfies the adjoint discrete equations

$$V^n = (A^n)^T V^{n+1},$$

subject to the final data

$$V_j^N = g(x_j).$$

The equivalence follows immediately from the identity

$$(V^0)^T U^0 = (V^N)^T A^{N-1} A^{N-2} \ldots A^1 A^0 U^0 = (V^N)^T U^N.$$

This adjoint approach to evaluating the output functional is advantageous when there is a single output functional of interest, but many different sets of initial data. Under these circumstances, the standard approach would require a separate forward analysis for each set of initial data, whereas the adjoint approach requires just one adjoint calculation, plus an inexpensive inner product evaluation for each set of initial data.

In the particular case of Dirac initial data with

$$U_j^0 \;=\; h^{-1}\delta_{j,0} \;\equiv\; \begin{cases} h^{-1}, & j = 0 \\ 0, & \text{otherwise} \end{cases}$$

one obtains

$$V_0^0 = h \sum_j g(x_j)\, U_j^N.$$

Thus, convergence of the integral output for Dirac initial data is equivalent to pointwise convergence of the adjoint discretisation. The results in this paper will be used in a future paper [7] to prove the pointwise convergence of adjoint discretisations when there are discontinuities in the solution of the underlying nonlinear p.d.e..

2   Fourier analysis of analytic problem

Fourier analysis will be used to analyse the discrete problem, so here we review the Fourier analysis of the analytic problem. The p.d.e. is

$$u_t = -a u_x + \epsilon u_{xx}, \quad a > 0,\ \epsilon > 0,$$

with initial data

$$u(x,0) = \delta(x).$$

The Fourier transform

$$\widehat{u}(\kappa, t) = \int_{-\infty}^{\infty} u(x,t)\, \exp(-\mathrm{i}\kappa x)\, \mathrm{d}x,$$

satisfies the equation

$$\widehat{u}_t = (-\mathrm{i}a\kappa - \epsilon\kappa^2)\, \widehat{u},$$

with initial data

$$\widehat{u}(\kappa, 0) = 1.$$

Hence,
$$\widehat{u}(\kappa, t) = \exp(-\mathrm{i}a\kappa - \epsilon\kappa^2)t,$$

and therefore
$$u(x,t) = \frac{1}{\sqrt{4\pi\epsilon t}} \exp \frac{(x-at)^2}{4\epsilon t} = \frac{1}{\sqrt{2\epsilon t}} \, N\left(\frac{x-at}{\sqrt{2\epsilon t}}\right),$$

where
$$N(x) = \frac{1}{\sqrt{2\pi}} \, \exp\left(-\frac{x^2}{2}\right),$$

is the standard normal distribution with zero mean and unit variance.

3   Fourier analysis of discrete approximation

The standard forward Euler central space discretisation on a uniform grid with spacing h and timestep k is

$$U_j^{n+1} = U_j^n - \frac{r}{2}\left(U_{j+1}^n - U_{j-1}^n\right) + d\left(U_{j+1}^n - 2U_j^n + U_{j-1}^n\right)$$

where
$$d = \frac{\epsilon k}{h^2}, \qquad r = \frac{ak}{h}.$$

The discrete approximation to the Dirac initial data is

$$U_j^0 \;=\; h^{-1}\delta_{j,0} \;\equiv\; \begin{cases} h^{-1}, & j = 0 \\ 0, & \text{otherwise.} \end{cases}$$

The aim of the convergence analysis is to find the l_∞ and l_1 norms of the error $U_j^n - u(x_j, t^n)$, defined as

$$\|U^n - u(\cdot, t^n)\|_{l_\infty} \;=\; \max_j \left|U_j^n - u(x_j, t^n)\right|,$$
$$\|U^n - u(\cdot, t^n)\|_{l_1} \;=\; h\sum_j \left|U_j^n - u(x_j, t^n)\right|,$$

at a fixed time $t^n = nk, n \geq 1$ as $h \to 0$ with d held fixed at a constant value $d < \frac{1}{2}$ for which the discretisation is stable for sufficiently small h. Initially, we will consider the particular case in which $\epsilon = 1$ and $t = 1$, and hence $r = a\,d\,h$. A similarity argument will then be used to extend the results to arbitrary values of both ϵ and t.

3.1   Unit viscosity Fourier analysis

To apply Fourier analysis, we first embed this problem within a semi-discrete problem by defining
$$\widehat{U}^0(\kappa) \;=\; H\left(\kappa + \tfrac{\pi}{h}\right) - H\left(\kappa - \tfrac{\pi}{h}\right) \;\equiv\; \begin{cases} 1, & |\kappa| < \pi/h \\ 0, & \text{otherwise} \end{cases}$$

for which the inverse Fourier transform gives

$$U^0(x) = \frac{\sin(\frac{\pi x}{h})}{\pi x} \equiv h^{-1}\text{sinc}\left(\frac{\pi x}{h}\right).$$

Note that $U^0(x_j) = U_j^0$, so these initial conditions have nodal values matching those of the discrete solution. The evolution of the semi-discrete solution is defined by the same finite difference equation,

$$
\begin{aligned}
U^{n+1}(x) = {} & U^n(x) - \frac{a\,d\,h}{2}\left(U^n(x+h) - U^n(x-h)\right) \\
& + d\left(U^n(x+h) - 2U^n(x) + U^n(x-h)\right),
\end{aligned}
$$

so it follows that $U^n(x_j) = U_j^n$ for all j, n.

The Fourier transform of this equation yields

$$\widehat{U}^n(\kappa) = z^n(\kappa)\,\widehat{U}^0(\kappa),$$

where

$$z(\kappa) = 1 - \mathrm{i}\,a\,d\,h\,\sin \kappa h - 4d\,\sin^2 \frac{\kappa h}{2}.$$

If we now define a new quantity $e(x)$ as

$$
\begin{aligned}
e(x) = {} & -\frac{d}{4\sqrt{2}}\,a^2 N''\left(\frac{x-a}{\sqrt{2}}\right) - \left(\frac{1}{24} - \frac{d}{4}\right) a N'''\left(\frac{x-a}{\sqrt{2}}\right) \\
& + \left(\frac{1}{48\sqrt{2}} - \frac{d}{8\sqrt{2}}\right) N''''\left(\frac{x-a}{\sqrt{2}}\right),
\end{aligned}
\tag{3.1}
$$

with Fourier transform

$$\widehat{e}(\kappa) = \left(\frac{d}{2}\,a^2\kappa^2 + \left(\frac{1}{6} - d\right)\mathrm{i}\,a\,\kappa^3 + \left(\frac{1}{12} - \frac{d}{2}\right)\kappa^4\right)\exp\left(-\mathrm{i}a\kappa - \kappa^2\right), \tag{3.2}$$

then the following lemma proves that $h^2\widehat{e}(\kappa)$ is the leading order term in the Fourier transform of the solution error at time $t=1$.

3.2 Analysis of Fourier transform error

Lemma 1 *Defining $r(x)$ through the error decomposition*

$$U^n(x) = u(x, 1) + h^2 e(x) + r(x),$$

for $n\,k = 1$, with $e(x)$ as defined in Equation (3.1), then for any $0 < d < \frac{1}{2}$ and $0 < m < \frac{1}{2}$, there exists $h_0(m) > 0$ such that for all $h < h_0(m)$ the Fourier transform $\widehat{r}(\kappa)$ satisfies the bounds

$$
|\widehat{r}(\kappa)| <
\begin{cases}
400\,h^4\left(|a\kappa|^3 + \kappa^6 + (a\kappa)^4 + \kappa^8\right)\exp(-\kappa^2), & |\kappa| \leq h^{-m}, \\[2mm]
\exp\left(-\dfrac{4\,(1-2d)\,\kappa^2}{\pi^2}\right) + \left(1 + h^2\left((a\kappa)^2 + \kappa^4\right)\right)\exp(-\kappa^2), & |\kappa| > h^{-m}.
\end{cases}
$$

Proof The proof has two parts, dealing with the two different ranges for κ.

i) $|\kappa| \leq h^{-m}$

An analytic function $f(\delta)$ has a truncated Taylor expansion of the form

$$f(\delta) = \sum_{p=0}^{n-1} \frac{\delta^p}{p!} f^{(p)}(0) + \frac{\delta^n}{n!} f_n, \qquad |f_n| \leq \sup_{|\xi| \leq \delta} |f^{(n)}(\xi)|. \tag{3.3}$$

The analysis now proceeds by using a sequence of three such expansions. Firstly, applying the expansion with $n=6$ to $z(h)$ gives

$$z = 1 + a_1 h^2 + a_2 h^4 + a_3 h^6,$$

where

$$
\begin{aligned}
a_1 &= \left(-\mathrm{i}\, a\, \kappa - \kappa^2\right) d, \\
a_2 &= \left(\tfrac{1}{6}\mathrm{i}\, a\, \kappa^3 + \tfrac{1}{12}\kappa^4\right) d, \\
|a_3| &\leq \left(\tfrac{1}{120}|a||\kappa|^5 + \tfrac{1}{360}\kappa^6\right) d.
\end{aligned}
$$

If h_0 is initially defined as $h_0 = (|a|+1)^{-1}$, then for $h < h_0$, $|\kappa| \leq h^{-m} \leq h^{-1}$, we have the inequalities

$$60\,|a_3|\, h^6 \leq 6\,|a_2|\, h^4 \leq |a_1|\, h^2 \leq d$$

and hence $|z| > \frac{1}{3}$.

Secondly, applying Equation (3.3) for $n=3$ to $f(\delta) = \log\left(1 + a_1\delta + a_2\delta^2 + a_3\delta^3\right)$, with a_3 treated as a constant not a function of δ, we obtain

$$
\begin{aligned}
f'(0) &= a_1, \\
f''(0) &= 2a_2 - a_1^2, \\
f'''(\delta) &= \frac{6a_3}{(1 + a_1\delta + a_2\delta^2 + a_3\delta^3)} - \frac{3(2a_2 + 6a_3\delta)(a_1 + 2a_2\delta + 3a_3\delta^2)}{(1 + a_1\delta + a_2\delta^2 + a_3\delta^3)^2} \\
&\qquad + \frac{2(a_1 + 2a_2\delta + 3a_3\delta^2)^3}{(1 + a_1\delta + a_2\delta^2 + a_3\delta^3)^3}.
\end{aligned}
$$

Setting $\delta = h^2$, then the inequalities above for a_1, a_2, a_3 imply that

$$\sup_{|\xi| \leq \delta} |f'''(\xi)| \leq 18\,|a_3| + 100\,|a_1 a_2| + 144\,|a_1|^3.$$

Hence, for $h < h_0$, $|\kappa| < h^{-m}$,

$$\log z = b_1 d h^2 + b_2 d h^4 + b_3 d h^6,$$

where

$$
\begin{aligned}
b_1 &= -\mathrm{i}\, a\, \kappa - \kappa^2, \\
b_2 &= \frac{d}{2} a^2 \kappa^2 + \left(\frac{1}{6} - d\right) \mathrm{i} a \kappa^3 + \left(\frac{1}{12} - \frac{d}{2}\right) \kappa^4, \\
|b_3| &\leq \frac{18\,|a_3| + 100\,|a_1 a_2| + 144\,|a_1|^3}{6d} \leq 40\left(|a\kappa|^3 + \kappa^6\right).
\end{aligned}
$$

From this it follows, using $nk = ndh^2 = 1$, that

$$n \log z = b_1 + b_2\,h^2 + b_3\,h^4,$$

and therefore

$$z^n = \exp(-\mathrm{i}\,a\,\kappa - \kappa^2)\,\exp(b_2\,h^2 + b_3\,h^4).$$

The restriction $0 < m < \frac{1}{2}$ ensures that both $b_2\,h^2$ and $b_3\,h^4$ are $o(1)$ as $h \to 0$ with $\kappa \le h^{-m}$. It is therefore possible to choose a new, smaller value for $h_0(m) > 0$ such that for all $h < h_0(m)$ and $\kappa \le h^{-m}$

$$|b_2|\,h^2 + |b_3|\,h^4 \le 1.$$

Finally, applying Equation (3.3) for $n = 2$ to $f(\delta) = \exp\big(b_2\delta + b_3\delta^2\big)$, with b_3 treated as a constant not a function of δ, we obtain

$$
\begin{aligned}
f'(0) &= b_2, \\
f''(\delta) &= \Big(2b_3(1 + 2b_2\delta + 2b_3\delta^2) + b_2^2\Big)\,\exp\big(b_2\delta + b_3\delta^2\big).
\end{aligned}
$$

Setting $\delta = h^2$, then the inequality above involving b_2 and b_3 implies that

$$\sup_{|\xi| \le \delta} |f''(\xi)| \le \big(6|b_3| + |b_2|^2\big)\,\exp(1).$$

Hence, for all $h < h_0(m)$ and $\kappa \le h^{-m}$

$$\exp\big(b_2\,h^2 + b_3\,h^4\big) = 1 + b_2 h^2 + b_4 h^4,$$

with

$$|b_4| \le 400\,\big(|a\kappa|^3 + \kappa^6 + (a\kappa)^4 + \kappa^8\big).$$

Thus, given the definition of $\widehat{e}(\kappa)$ in Equation (3.2),

$$
\begin{aligned}
z^n &= \exp(-\mathrm{i}\,a\,\kappa - \kappa^2)\,\big(1 + b_2 h^2 + b_4 h^4\big) \\
&= \widehat{u}(\kappa, 1) + h^2\widehat{e}(\kappa) + b_4 h^4 \exp(-\mathrm{i}\,a\,\kappa - \kappa^2),
\end{aligned}
$$

and the upper bound on $|b_4|$ gives the desired result.

ii) $|\kappa| > h^{-m}$

Since $|a|\,h_0(m) < 1$, then for $|\kappa| > h^{-m}$, $h < h_0(m)$,

$$
\begin{aligned}
|z|^2 &= 1 - 8d\,\sin^2\frac{\kappa h}{2}\left(1 - 2d\sin^2\frac{\kappa h}{2} - \tfrac{1}{2}(ah)^2 d\cos^2\frac{\kappa h}{2}\right) \\
&\le 1 - 8\,d(1 - 2d)\,\sin^2\frac{\kappa h}{2}.
\end{aligned}
$$

Since $\sin^2(\theta/2) \ge (\theta/\pi)^2$ for $\theta \in [0, \pi]$, it follows that for $|\kappa| \le \pi/h$,

$$|z|^2 \le 1 - \frac{8\,d(1-2d)\,\kappa^2 h^2}{\pi^2} \le \exp\left(-\frac{8\,d(1-2d)\,\kappa^2 h^2}{\pi^2}\right),$$

and hence for fixed $nk = ndh^2 = 1$ we obtain

$$|\widehat{U}^n(\kappa)| \le \exp\left(-\frac{4\,(1-2d)\,\kappa^2}{\pi^2}\right).$$

Note that this inequality is also trivially satisfied for $|\kappa| > \pi/h$ since $\widehat{U}^n(\kappa)$ is identically zero.

In addition,

$$|\widehat{u}(\kappa, 1)| = \exp(-\kappa^2),$$

and

$$|\widehat{e}(\kappa)| < \left((a\kappa)^2 + \kappa^4\right) \exp(-\kappa^2).$$

Since

$$\widehat{r}(\kappa) = \widehat{U}^n(\kappa) - \widehat{u}(\kappa, 1) - h^2 \widehat{e}(\kappa),$$

it therefore follows that

$$|\widehat{r}(\kappa)| < \exp\left(-\frac{4(1-2d)\kappa^2}{\pi^2}\right) + \left(1 + h^2\left((a\kappa)^2 + \kappa^4\right)\right)\exp(-\kappa^2).$$

∎

3.3 l_∞ and l_1 error estimates

The lemma in the previous section derived a representation of the Fourier transform of the discretisation error. We now use the inverse Fourier transform to bound $r(x)$.

Using the notation $q(h) \simeq p(h)$ to denote that

$$\frac{q(h)}{p(h)} - 1 = o(h), \text{ as } h \to 0,$$

then the main theorem of this paper is as follows:

Theorem 2 *If $r(x)$ is as defined in Lemma 3.1, then*

$$\|r\|_{L_\infty} = O(h^4),$$

and

$$\|r\|_{l_1} = O(h^3),$$

and hence

$$\|U^n - u(\cdot, 1)\|_{l_\infty} \simeq h^2 \|e\|_{L_\infty},$$

and

$$\|U^n - u(\cdot, 1)\|_{l_1} \simeq h^2 \|e\|_{L_1},$$

except for the specific case $a = 0$, $d = \frac{1}{6}$ for which $e(x)$ is identically zero.

Proof

$$r(x) = \frac{1}{2\pi} \int_{-\infty}^{\infty} \widehat{r}(\kappa) \exp(i\kappa x) \, d\kappa,$$

so

$$|r(x)| \leq \frac{1}{2\pi} \int_{-\infty}^{\infty} |\widehat{r}(\kappa)| \, d\kappa.$$

Choosing any $0 < m < \frac{1}{2}$, and introducing the bounds on $|\widehat{r}(\kappa)|$ from Lemma 3.1 gives

$$
\begin{aligned}
|r(x)| \;\leq\; & \frac{400\,h^4}{2\pi} \int_{-\infty}^{\infty} \left(|a\kappa|^3 + \kappa^6 + (a\kappa)^4 + \kappa^8 \right) \exp(-\kappa^2)\,\mathrm{d}\kappa \\
& + \frac{1}{\pi} \int_{h^{-m}}^{\infty} \exp\left(-\frac{4\,(1-2d)\,\kappa^2}{\pi^2} \right) + \left(1 + h^2\left((a\kappa)^2 + \kappa^4 \right) \right) \exp(-\kappa^2)\,\mathrm{d}\kappa,
\end{aligned}
$$

for $h < h_0(m)$. The first of the above integrals is finite, and the second is $o(h^4)$ due to Lemma A.1 in the Appendix. Hence, $\|r\|_{L_\infty} = O(h^4)$.

Bounding $\|r(x_j)\|_{l_1}$ requires consideration of two contributions, from inside and outside the interval $[-nh, nh] = [-h^{-1}, h^{-1}]$. Within the interval,

$$
h \sum_{|j| \leq n} |r(x_j)| \;\leq\; (2n+1)\,h\,\|r\|_{L_\infty} = O(h^3).
$$

Outside the interval $[-h^{-1}, h^{-1}]$, U_j^n is identically zero due to the explicit nature of the discretisation and the finite domain of influence associated with the Dirac initial data. Also, outside this interval $u(x,1)$, $e(x)$ and their derivatives and total variation are all $o(h^p)$ for any $p > 1$. Hence, again using the integral bounds in Lemma A.1,

$$
\begin{aligned}
h \sum_{|j| > n} \left| r(x_j) \right| \;=\; & h \sum_{|j| > n} \left| u(x_j, 1) + h^2 e(x_j) \right| \\
\leq\; & \int_{-\infty}^{-h^{-1}} |u(x,1) + h^2 e(x)|\,\mathrm{d}x + \int_{h^{-1}}^{\infty} |u(x,1) + h^2 e(x)|\,\mathrm{d}x \;+\; o(h^3) \\
=\; & o(h^3).
\end{aligned}
$$

Combining the contributions from inside and outside the interval $[-h^{-1}, h^{-1}]$ proves that $\|r(x_j)\|_{l_1} = O(h^3)$.

The final step, obtaining the asymptotically sharp error estimates, comes from the fact that

$$
U_j^n - u(x_j, 1) = h^2 e(x_j) + r(x_j)
$$

and so therefore, by the triangle inequality,

$$
h^2 \|e\|_{l_\infty} - \|r\|_{l_\infty} \;\leq\; \|U^n - u(\cdot, 1)\|_{l_\infty} \;\leq\; h^2 \|e\|_{l_\infty} + \|r\|_{l_\infty},
$$

$$
h^2 \|e\|_{l_1} - \|r\|_{l_1} \;\leq\; \|U^n - u(\cdot, 1)\|_{l_1} \;\leq\; h^2 \|e\|_{l_1} + \|r\|_{l_1}.
$$

The proof is completed by noting that $\|r\|_{l_1}$ and $\|r\|_{l_\infty}$ are both $o(h^2)$, and $\|e\|_{l_\infty} = \|e\|_{L_\infty} + O(h)$, and $\|e\|_{l_1} = \|e\|_{L_1} + O(h)$, since $e(x)$ has a bounded derivative and has bounded variation. ∎

3.4 Extension to arbitrary viscosity and time

Suppose now that one is interested in the error at time $t = T$, arising from the discretisation

$$
U_j^{n+1} = U_j^n - \frac{r}{2}\left(U_{j+1}^n - U_{j-1}^n \right) + d\left(U_{j+1}^n - 2U_j^n + U_{j-1}^n \right)
$$

with

$$d = \frac{\epsilon k}{h^2}, \qquad r = \frac{ak}{h},$$

and initial data

$$U_j^0 = h^{-1}\delta_{j,0} \equiv \begin{cases} h^{-1}, & j = 0 \\ 0, & \text{otherwise} \end{cases}$$

Making the substitutions

$$\bar{t} = \frac{t}{T}, \qquad \bar{x} = \frac{x}{\sqrt{\epsilon T}}, \qquad \bar{a} = a\sqrt{\frac{T}{\epsilon}},$$

$$\bar{k} = \frac{k}{T}, \qquad \bar{h} = \frac{h}{\sqrt{\epsilon T}}, \qquad \bar{U}_j^n = \sqrt{\epsilon T}\, U_j^n,$$

leads to the finite difference equation

$$\bar{U}_j^{n+1} = \bar{U}_j^n - \frac{\bar{r}}{2}(\bar{U}_{j+1}^n - \bar{U}_{j-1}^n) + \bar{d}(\bar{U}_{j+1}^n - 2\bar{U}_j^n + \bar{U}_{j-1}^n)$$

with

$$\bar{d} = \frac{\bar{k}}{\bar{h}^2} = d, \qquad \bar{r} = \frac{\bar{a}\bar{k}}{\bar{h}} = r,$$

and initial data

$$\bar{U}_j^0 = \bar{h}^{-1}\delta_{j,0} \equiv \begin{cases} \bar{h}^{-1}, & j = 0 \\ 0, & \text{otherwise} \end{cases}$$

with the error being considered at time $\bar{t} = 1$, as analysed previously.

Hence, the l_∞ and l_1 error estimates for the general problem at fixed time $t = nk$, $n \geq 1$, are given by the following corollary.

Corollary 2A *For the discretisation of the general problem described above, with fixed $d < \frac{1}{2}$,*

$$\left\| U^n - u(\cdot, t) \right\|_{l_\infty} \simeq \frac{1}{\sqrt{\epsilon t}} \frac{h^2}{\epsilon t} \left\| e(\cdot, t) \right\|_{L_\infty}, \tag{3.4}$$

and

$$\left\| U^n - u(\cdot, t) \right\|_{l_1} \simeq \frac{h^2}{\epsilon t} \left\| e(\cdot, t) \right\|_{L_1}, \tag{3.5}$$

where

$$\begin{aligned} e(x, t) &= -\frac{d}{4\sqrt{2}} \frac{a^2 t}{\epsilon} N''\left(\frac{x}{\sqrt{2}}\right) \\ &\quad - \left(\frac{1}{24} - \frac{d}{4}\right) \sqrt{\frac{a^2 t}{\epsilon}} N'''\left(\frac{x}{\sqrt{2}}\right) \\ &\quad + \left(\frac{1}{48\sqrt{2}} - \frac{d}{8\sqrt{2}}\right) N''''\left(\frac{x}{\sqrt{2}}\right), \end{aligned}$$

except for the specific case $a = 0$, $d = \frac{1}{6}$ for which $e(x, t)$ is identically zero.

4   Numerical results

Here we show numerical results on the domain $-10 < x < 10$ and the time interval $0 < t < 1$. All of the results use $\epsilon = 1$ and timestep $k = dh^2$ with $d = 1/8$.

The first two figures present results over the whole time interval, using a fixed grid with spacing $h = 0.02$. Figure 1 presents results for the diffusion equation with $a = 0$. Figure 1a shows the numerical solution at $t = 0.2, 0.4, 0.6, 0.8, 1.0$. Figure 1b presents the l_∞ and l_1 solution errors versus time t, and Figure 1c presents the same errors normalised by the asymptotic estimates given in Equations (3.4) and (3.5). It is apparent that the asymptotic estimates very accurately approximate the actual error, once t is sufficiently large so that $h^2/t \ll 1$.

It is worth commenting on the lack of smoothness in the error/estimate curves. In the case of the l_∞ error, this is due to changes in the location of the node for which the error is maximum. Similarly, for the l_1 error it is due to sign changes in the error at specific nodes as time increases.

Figure 2 presents the corresponding results for the convection/diffusion equation with $a = 2$. Again the asymptotic estimates very accurately approximate the actual error. Note also that the errors are much larger than in the case of pure diffusion, with the l_1 error approaching a constant value equal to

$$\frac{da^2 h^2}{4\,\epsilon^2}\, \|N''\|_{L_1} = \frac{d}{\sqrt{2\pi e}} \left(\frac{ah}{\epsilon} \right)^2 .$$

Figures 3 and 4 present convergence results showing how the error at the final time $t = 1.0$ varies with grid spacing h. Figure 3 has the results for the diffusion equation with $a = 0$. Figure 3a shows the numerical solution on the finest grid with $h = 0.02$. Figure 3b presents the l_∞ and l_1 errors, and Figure 3c presents the same errors normalised by the asymptotic estimates given in Equations (3.4) and (3.5). Figure 4 has the corresponding results for the convection/diffusion equation with $a = 2$.

5   Conclusions

In this paper we have derived sharp estimates for the error arising from a particular explicit discretisation of the constant coefficient 1D convection/diffusion equation subject to Dirac initial data. Extending the analysis to other linear explicit and implicit discretisations would be straightforward. The extension of the Fourier analysis to multiple dimensions would also pose no difficulties.

To extend the analysis to varying coefficients would not be so easy, but could be performed using a matched inner and outer asymptotic analysis, with the inner analysis in the neighbourhood of the Dirac initial data being performed using the analysis in this paper, treating the coefficients as being locally approximately constant. The inner solution would then have to be matched to an outer solution describing the subsequent evolution of the solution and the discretisation error in the outer region in which the solution is well resolved, at least asymptotically.
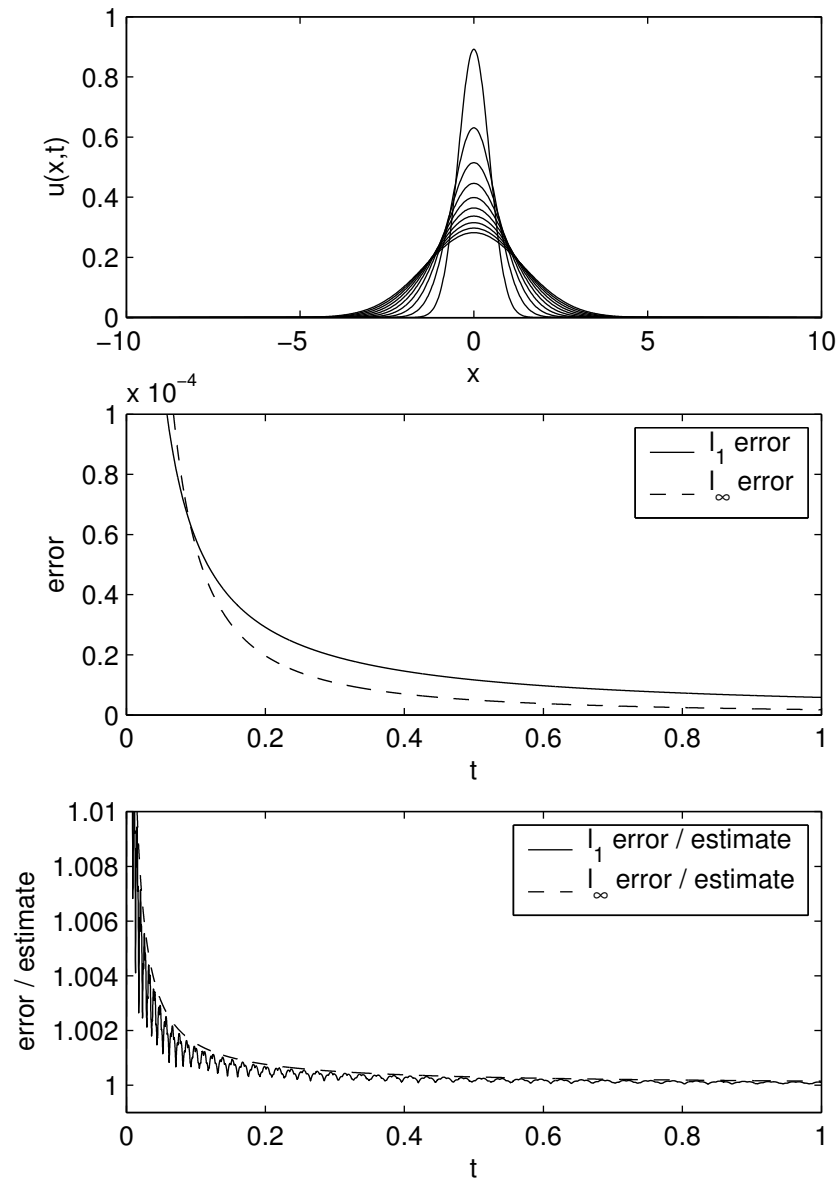
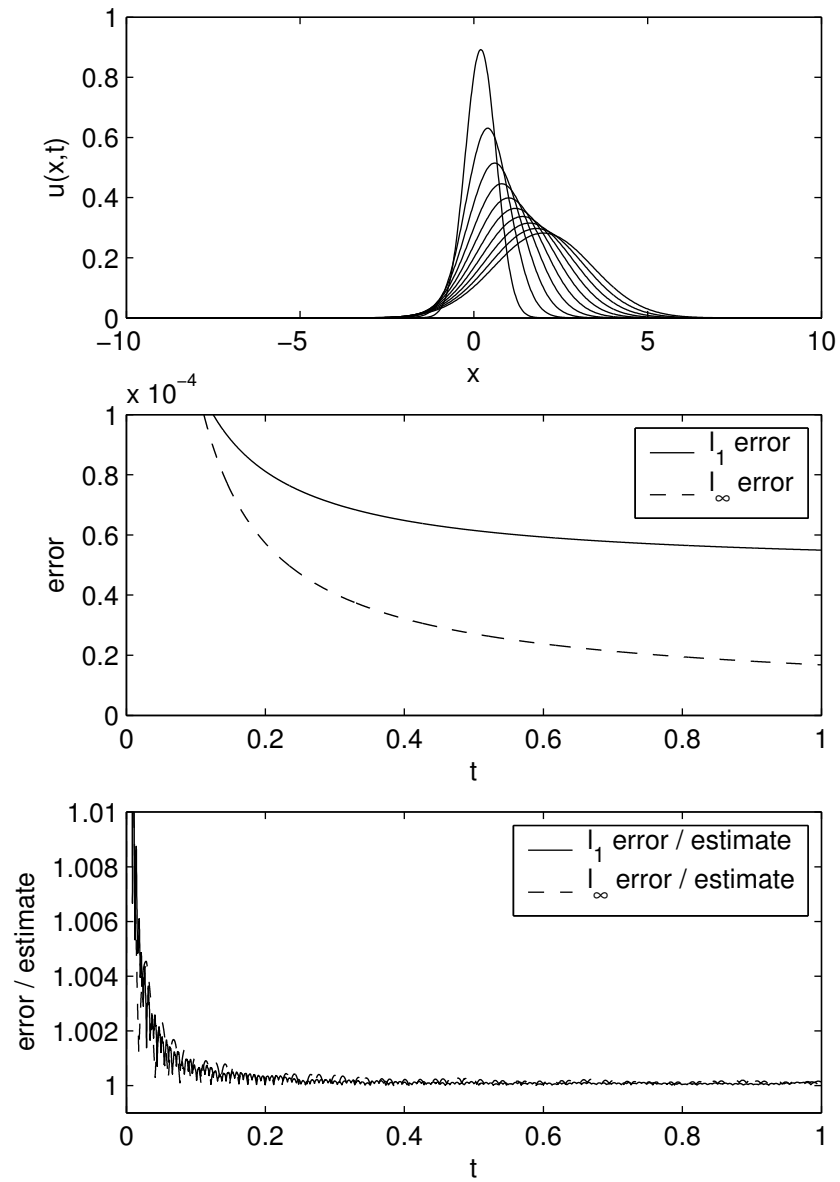Figure 1: Numerical results for the diffusion equation

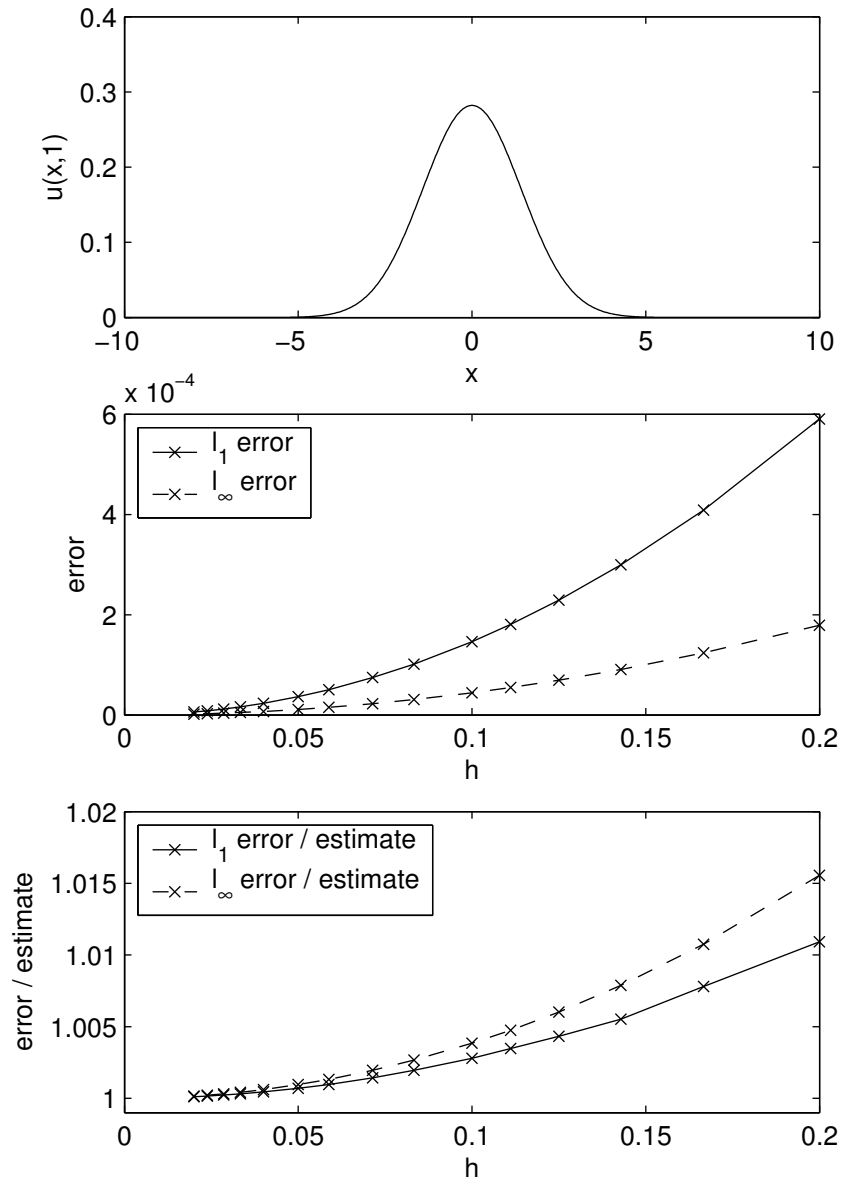Figure 2: Numerical results for the convection/diffusion equation

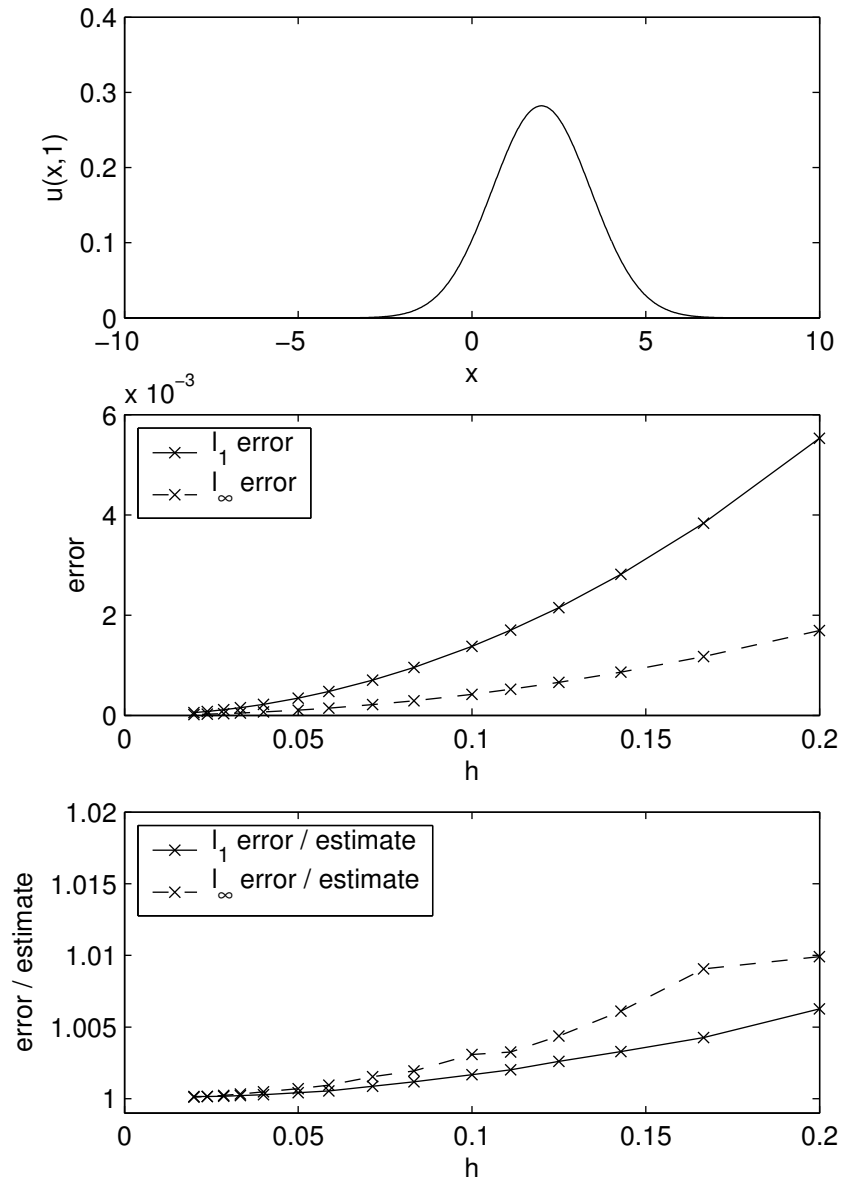Figure 3: Convergence results for the diffusion equation

Figure 4: Convergence results for the convection/diffusion equation

The results in this paper can also be used in circumstances where ϵ depends on the mesh spacing h, provided $\bar{h} = h/\sqrt{\epsilon t} \to 0$. This is important in proving the pointwise convergence of adjoint Burgers equation solutions along characteristics leading into a discontinuity in the underlying nonlinear solution [7].

Acknowledgements

Appendix A   Some integral bounds

Lemma 3 *For any integers $p > 0$ and $n \geq 0$,*

$$\int_V^\infty v^n \, \exp(-v^2) \, \mathrm{d}v = o(V^{-p}), \quad as \ V \to \infty.$$

Proof The proof is by induction on n. If the proposition is true for $n \geq 0$, then integration by parts gives

$$\int_V^\infty v^{n+2} \, \exp(-v^2) \, \mathrm{d}v = \frac{1}{2} \, V^{n+1} \, \exp(-V^2) + \frac{n+1}{2} \int_V^\infty v^n \, \exp(-v^2) \, \mathrm{d}v,$$

and hence it is also true for $n+2$.

The proof is completed by noting that for $n = 0$, and $V > 0$,

$$\int_V^\infty \exp(-v^2) \, \mathrm{d}v \leq \int_V^\infty \exp(-vV) = \frac{1}{V} \, \exp(-V^2) = o(V^{-p}),$$

while for $n = 1$,

$$\int_V^\infty v \, \exp(-v^2) \, \mathrm{d}v = \frac{1}{2} \, \exp(-V^2) = o(V^{-p}).$$

■

Appendix References

[1] T. Barth and H. Deconinck, editors. *Error Estimation and Adaptive Discretization Methods in Computational Fluid Dynamics.* Number 25 in Lecture Notes in Computational Science and Engineering. Springer-Verlag, 2002.

[2] R. Becker and R. Rannacher. An optimal control approach to error control and mesh adaptation. In A. Iserles, editor, *Acta Numerica 2001.* Cambridge University Press, 2001.

[3] P. Brenner, V. Thomée, and L. Wahlbin. *Besov spaces and applications to difference methods for initial value problems.* Number 434 in Lecture Notes in Mathematics. Springer Verlag, 1975.

[4] D. Darmofal and D. Venditti. Anisotropic grid adaptation for functional outputs: application to two-dimensional viscous flows. *Journal of Computational Physics*, 187:22–46, 2003.

[5] M.B. Giles. Discrete adjoint approximations with shocks. In T. Hou and E. Tadmor, editors, *Hyperbolic Problems: Theory, Numerics, Applications.* Springer-Verlag, 2003.

[6] M.B. Giles and E. Süli. Adjoint methods for PDEs: *a posteriori* error analysis and postprocessing by duality. In A. Iserles, editor, *Acta Numerica 2002*, pages 145–236. Cambridge University Press, 2002.

[7] M.B. Giles and S. Ulbrich. Convergence of discrete linearised and adjoint approximations in the presence of a shock. In preparation, 2004.

[8] A. Jameson. Aerodynamic design via control theory. *Journal of Scientific Computing*, 3:233–260, 1988.

[9] A. Jameson, N. Pierce, and L. Martinelli. Optimum aerodynamic design using the Navier-Stokes equations. *Journal of Theoretical and Computational Fluid Mechanics*, 10:213–237, 1998.

[10] N.A. Pierce and M.B. Giles. Adjoint recovery of superconvergent functionals from PDE approximations. *SIAM Review*, 42(2):247–264, 2000.

[11] S. Ulbrich. A sensitivity and adjoint calculus for discontinuous solutions of hyperbolic conservation laws with source terms. *SIAM Journal of Control and Optimization*, 41(3):740–797, 2002.

[12] S. Ulbrich. Adjoint-based derivative computations for the optimal control of discontinuous solutions of hyperbolic conservation laws. *Systems & Control Letters*, 48(3-4):313–328, 2003.